Theory of morphological transformation of viral capsid shell during the maturation process in the HK97 bacteriophage and similar viruses

O. V. Konevtsova, V. L. Lorman, and S. B. Rochal

Phys. Rev. E **93**, 052412 — Published 19 May 2016

DOI: 10.1103/PhysRevE.93.052412

Theory of morphological transformation of viral capsid shell during the maturation process in the HK97 bacteriophage and similar viruses

O.V. Konevtsova,[*] V.L. Lorman,[†] and S.B. Rochal[*]

[*]Faculty of Physics, Southern Federal University, 5 Zorge str., 344090 Rostov-on-Don, Russia
[†]Laboratoire Charles Coulomb, UMR 5221 CNRS and Université de Montpellier, pl. E. Bataillon, 34095 Montpellier, France

We consider the symmetry and physical origin of collective displacement modes playing a crucial role in the morphological transformation during the maturation of the HK97 bacteriophage and similar viruses. It is shown that the experimentally observed hexamer deformations and pentamer twists in the HK97 procapsid correspond to the simplest irreducible shear strain mode of a spherical shell in the continuous approximation. We also show that the icosahedral faceting of the bacteriophage capsid shell is driven by the simplest irreducible radial displacement field. The shear field has the rotational icosahedral symmetry group I while the radial field has the full icosahedral symmetry I_h. This difference makes their actions independent. The radial field sign discriminates between the icosahedral and the dodecahedral shapes of the faceted capsid shell, thus making the approach relevant not only for the HK97-like viruses but also for the Parvovirus family. In the frame of the Landau-Ginzburg formalism we propose a simple phenomenological model valid for the first reversible step of the HK97 maturation process. The calculated phase diagram illustrates the discontinuous character of the virus shape transformation. The characteristics of the virus shell faceting and expansion obtained in the *in vitro* and *in vivo* experiments are related to the decrease in the capsid shell thickness and to the increase of the internal capsid pressure.

PACS numbers: 62.23.St, 64.70.Nd, 87.15.Zg

I. INTRODUCTION

Self-assembly and shape transitions in biological nanostructures with non-trivial topology are characterized by unconventional properties and unusual pathways. In contrast to classical condensed matter, bionanoassemblies undergo a multistep process which involves several physical transformations. Virus self-assembly is a typical example of a multistep process of this type [1]. Viral capsid, the protein shell which protects viral genome, passes through several successive steps of the assembly process. At the first step the so-called procapsid shell self-assembles from the aqueous solution of individual viral proteins. The process called capsid maturation is the final step of the virus self-assembly. During maturation the virus acquires the ability to infect the host cell. The process is characterized by a number of considerable correlated structure changes in the procapsid shell resulting in the mature infectious virion.

One of the most interesting features of the maturation process in a variety of viruses is a morphological transformation of the capsid shell resulting in a shape transition from the *spherical* to the *faceted* polyhedral geometry. It is worth noting that maturation in the host cell secretory pathway is often accompanied by irreversible biochemical events in capsid proteins including protein domain cleavage or neighboring protein cross-linking [2,3]. However, irreversible events usually take place at the stages of the maturation process different from the stage of the structural modification leading to final protein positions and orientations in the shell (see e.g. [4]). Direct *in vivo* experiments [4] evidenced this fact and allowed the authors of [4] to

perform the *in vitro* structural procapsid-to-capsid transformation of a complex virus in a reversible and perfectly controlled manner. They have shown that the reversible structural transition during the maturation process can be considered as an independent physical phenomenon. This fact makes it possible to treat the reversible stage of the maturation process within the general frame of condensed matter physics.

To illustrate the notions of the theory developed in our work we choose the example of bacteriophage HK97. Other viruses with similar structural characteristics can be considered in the same framework. The HK97 bacteriophage is a dsDNA virus with the icosahedral capsid protein shell. The protein density in the capsid has the rotational icosahedral symmetry group *I* and consists of 420 proteins distributed in seven 60-fold general positions of this group. The capsid structure satisfies to the well-known Caspar and Klug geometrical model [5] which limits the number of proteins constituting the shell to N=60T where the number of different positions T takes the value $T = h^2 + k^2 + hk$, with h and k being non-negative integers. The eventful maturation scenario of the HK97 bacteriophage is studied in detail by high-resolution structural methods. The morphological transformation of the *spherical* procapsid into the *faceted* capsid during the HK97 maturation process is accompanied by a strong increase in the shell volume and in the mean capsid diameter [6,7]. The diameter undergoes a growth of about 20%. The protein-shell wall becomes much thinner, the shell thickness becomes more homogeneous, and, finally, the shell acquires a pronounced *icosahedral shape*. The multistep maturation process with a faceting transition at its intermediate stages is typical not only for the HK97 bacteriophage, but for a variety of viruses (e.g. P22 phage, Herpes Simplex Virus, etc.) with similar structural organization [8].

The morphological changes at different steps of the HK97 maturation process are observed in both *in vivo* and *in vitro* experiments. On the one hand, in the host cell pathway these morphological changes are induced by the intracellular pH-level gradient and by the ATP-dependent genome packaging into the pre-assembled procapsid protein shell. On the other hand, in *in vitro* experiments the same structure and shape variation are reproduced in the absence of viral genomic DNA, by using the controlled pH decrease of the buffer [8]. Intermediate steps of the HK97 bacteriophage maturation *in vivo* are practically inaccessible experimentally while *in vitro* experiments provide the information which is still not complete. The structures of the procapsid and matured capsid shells are usually determined by means of X-ray crystallography and high-resolution cryoelectron microscopy (cryoEM) [7,9]. It is difficult to obtain from these data the information about the intermediate states of the *in vivo* maturation process. Biochemical *in vitro* experiments study maturation dynamics in the buffers with controlled pH level [10,11] and manage to distinguish several intermediate states with the faceted capsid shells and one intermediate state with the spherical shape symmetry. The intermediate states are stabilized at different pH levels and are characterized by successive increase in the shell volume.

Reversibility of the processes taking place at different steps of the structural transformation during the HK97 maturation was discussed in a series of previous works [10,12-15]. In our opinion, the most realistic scheme of the maturation process, which clearly indicates the reversible and the irreversible steps, was given in [12]. The transition between the spherical procapsid (Prohead-II) and the flattened Expansion Intermediate (EI) state was shown to be reversible in [10]. Reversibility of maturation steps is often investigated using the HK97 bacteriophage mutants exhibiting no protein cross-linking. In this case even the transformation between the EI and the so-called Balloon state is reversible [12]. The next stage of the *in vitro* process, i.e. the Balloon-to-Head II transformation was also found reversible in [13]. However, these results are in contradiction with the data obtained by [14] indicating that the Balloon-to-Head transition is not readily reversible, even in the absence of crosslinks. Note also that at T>54°C the transformation between the spherical procapsid (Prohead I) and the flattened Expanded Prohead I states is reversible in *in vitro* experiments [15]. Thus, the HK97

bacteriophage represents an example of a virus with the structural transformation during maturation process that can be studied within the frame of well-established physical methods.

In spite of the progress in experimental studies the relation between the pH-induced structure variation in *in vitro* experiments and the *in vivo* capsid transformations induced by the genome packaging with the help of motor proteins [3] remains unclear. It is still difficult to characterize virus maturation dynamics and kinetics experimentally. This situation renders the predictions of theoretical and numerical modeling essential for the understanding of the procapsid shell transformation into the mature infectious virion.

Several models have been proposed to approach theoretically the HK97 capsid morphological transformation [16-20]. Structural changes during maturation have been described in [16] as a condensation of several low-frequency modes in a model system with the icosahedral symmetry. Two types of modes were considered to be responsible for the capsid faceting, the modes of the capsid isotropic expansion (or compression) and the modes of the pentamer displacements. The HK97 virus maturation was also modeled [17] in the frame of the simplified Landau-Ginzburg theory of phase transitions. In contrast with the classical Landau-Ginzburg approach, the model proposed in [17] did not take into account the normal mode symmetry. In this simplified approach the order parameter was taken as a scalar physical quantity. Thus, this approximation has disconnected the free energy of the model from the capsid structure and symmetry characteristics. At the same time additional terms dependent on continuous derivatives of the order parameter with respect to the variables on the shell surface were introduced in the free energy, though the shell consists of only 420 particles. The intermediate structures of the maturation process obtained in the frame of this approach are spatially inhomogeneous and their interpretation on the basis of available experimental data is not straightforward. The model [17] was then modified [18] by introducing the methods of continuum elasticity theory but still remained disconnected from the mode symmetry.

The present work aims to provide a detailed group theory analysis of the critical modes responsible for the morphological changes in the HK97 bacteriophage, and to propose a minimal model of the procapsid-to-capsid transformation. The model is developed in the frame of the Landau-Ginzburg approach with the well-defined physical meaning of the free energy terms.

The paper is organized as follows. In section II we show that all basic morphological changes of the HK97 protein shell during the maturation process are related to the well-defined normal modes of a homogeneous spherical membrane. We clarify the roles of the global expansion mode and of the shape symmetry-breaking mode responsible on the shell faceting. In addition, we explain how the simplest irreducible global shear strain mode of the spherical membrane induces the experimentally observed hexamer distortions and pentamer rotations. We elucidate the found relation between the global shear mode and the local distortions which is not obvious and was never discussed previously. A thermodynamic model of the capsid transformation is developed in the third section. The proposed theory is applicable to a variety of viruses demonstrating the maturation process accompanied by a capsid faceting and a discontinuous volume jump.

II. CRITICAL ORDER PARAMETERS RESPONSIBLE FOR THE MORPHOLOGICAL TRANSFORMATION

As it was shown previously in [16], the structural changes during maturation in the capsid shell of the HK97 bacteriophage, and in capsids of several similar viruses, involve two coupled low-frequency modes. First of them induces an isotropic capsid expansion, the second one is responsible for the shell faceting. Let us discuss the symmetry characteristics of the capsid protein shell and their incidence on the modes responsible for the morphological changes during the maturation process. Note that the symmetry of the microscopic protein *density distribution*

differs from the macroscopic symmetry of the shell *shape*. During the morphological procapsid-to-capsid transformation the protein distribution symmetry remains unchanged though the symmetry of the shell shape changes. Due to the asymmetry (and namely to the chirality) of coat proteins the protein density distribution in both the procapsid and the capsid states have the same chiral symmetry group I of all icosahedral rotations [5,21]. In contrast, the 2D shell shape is given by a regular system of points in the 3D space and is independent on the symmetry of individual proteins. The shape of the procapsid shell with the icosahedral density distribution is spherical with a good accuracy. During the morphological transformation the capsid shell acquires icosahedral faceted shape with the average macroscopic symmetry of the I_h group, which contains all symmetries of an icosahedron including spatial inversion and mirror planes. The displacement field relating the spherical procapsid and the icosahedral capsid shell shapes also has the average macroscopic symmetry given by the I_h group. This field is evidently invariant with respect to the spatial inversion operation. Consequently, the modes responsible on the transformation should be classified according to the sphere symmetry group O(3) which contains spatial inversion (in contrast with the SO(3) group).

Different modes of a spherical membrane with the O(3) symmetry are classified according to irreducible representations (IRs) of this group. Three types of modes are usually distinguished, bending, stretching and shear. In contrast to the case of the planar membrane, bending and stretching modes of the spherical membrane can be strongly coupled. It is the case of the bending and stretching modes with the same wave number l which form two linearly coupled bending-stretching modes. The displacement field corresponding to each coupled bending-stretching mode contains both radial and tangent components. On the contrary, the symmetry of the shear mode differs from the symmetry of the bending-stretching mode with the same wave number l, and the shear displacement field has the tangent component only. Due to the symmetry difference the shear field is linearly *independent* from the bending-stretching modes.

Linearly coupled bending-stretching modes can be classified in a function of the relative contribution of radial and tangent components in the mode amplitude. The mode with the main contribution of the radial component can be conventionally called “bending” of the spherical membrane. On the one hand, the mode with the main tangent contribution can play the role of “stretching”. It is the *radial* displacement field which brings the main contribution to the spherical membrane *shape* variation (for the full mode classification and detailed study of the corresponding mechanical problem see [22]). Consequently, the main shape changes in the viral capsid during its maturation process are related to the shape variation induced by the radial displacement field component. The stretching component of the displacement field spans the same irreducible representation of the O(3) group as the radial component does, and, consequently, its amplitude is directly determined by the coupling with the radial component. Thus, we start our symmetry analysis with the radial displacement field component.

Any radial displacement field of the spherical membrane is expanded in scalar spherical harmonics:

$$u_r(\theta,\phi) = \sum_{l=0}^{\infty} \sum_{l=-m}^{l=m} A_{l.m} Y_{l.m}(\theta,\phi), \tag{1}$$

where θ and ϕ are the angles of a standard spherical coordinate system. Corresponding Cartesian vector **R’** of a point on the deformed sphere surface has the form:

$$\mathbf{R}' = <(u_r + R)\sin\theta\cos\phi, (u_r + R)\sin\theta\sin\phi, (u_r + R)\cos\theta>, \tag{2}$$

where R is the radius of the initial non-deformed sphere. The normal mode responsible for the shape symmetry breaking spans the irreducible representation of the O(3) group labeled by a fixed value of the wave number l.

The spherical harmonic Y_{00} describes an isotropic expansion (or compression) of the procapsid shell and plays the role of the first one-dimensional fully symmetrical order parameter of the minimal model developed in our approach. The second order parameter responsible for the shape variation from the spherical to the icosahedral one is not so simple, and needs much more detailed discussion. Because of the shape invariance with respect to spatial inversion, expansion (1) is limited to the spherical harmonics with *even* wave numbers *l* only. Furthermore, there are additional drastic rules which select possible *l* values for the irreducible modes which can drive the transition from the spherical shape to the shape with the full icosahedral symmetry I_h. The analysis based on the invariant theory (see Appendix) shows that these modes correspond to the functions $Y_{l.m}(\theta,\phi)$ with the wave numbers *l* satisfying the following selection rules:

$$l = 6i + 10j\,, \tag{3}$$

where *i* and *j* are positive integers or zero. The sequence *L* of the wave number *l* values ($l \in L$) allowed by (3) has the form: *L* = (6, 10, 12, 16, 18, 20, 22, 24 ...). It selects the spherical harmonics, and, consequently, the symmetry breaking modes which can give a contribution to icosahedral faceting of the spherical viral capsid.

The explicit form of the displacement field $u_r(\theta,\phi)$ in the state with the icosahedral shape is obtained in terms of orthogonal icosahedral functions $f_l^i(\theta,\varphi)$ with the full icosahedral symmetry

$$u_r(\theta,\phi) = A_{0.0} + \sum_{l\in L}\sum_{i=1}^{i=n_t} D_{l.i} f_l^i(\theta,\phi), \tag{4}$$

where $D_{l,i}$ are the amplitudes of the functions. The index *i* (*i*=1,…, n_t) in Eq. (4) runs over all functions with the same fixed wave number *l*. The number of n_t values is equal to the number of non-negative integer solutions (*i*, *j*) of equation (3) for a given allowed value of *l*. Consequently, the number of linearly independent icosahedral functions $f_l^i(\theta,\varphi)$ is quite limited. According to Eq. (3) this number is equal to $n_t = 1$ for all *l*<30. The explicit form of the icosahedral functions $f_l^i(\theta,\varphi)$ with a given fixed *l* value is easily obtained by the averaging of spherical harmonics Y_{lm} over the full icosahedral symmetry group I_h:

$$f_l^i(\theta,\varphi) = C_l^i \sum_G Y_{lm}(\hat{g}(\theta,\varphi)), \tag{5}$$

where $G=I_h$ and the coefficients C_l^i can be determined from the normalization and (for $l\geq 30$) from the orthogonality condition for functions (5) with the same *l* value.

Number n_t can also be obtained by a classical method widely used in condensed matter physics, especially in Raman and IR spectroscopies for the active mode determination [23]. It is based on the well-known character relation of the representations for the symmetry groups of the symmetric state and the state with the broken symmetry (i.e. the state with non-zero mode amplitude). For the procapsid spherical shell the harmonics $Y_{l.m}(\theta,\phi)$ with *m*=-*l*, -*l*+1, ... *l* span one (2*l*+1)–dimensional irreducible representation of the O(3) group. The icosahedral functions $f_l^i(\theta,\varphi)$ introduced above form an orthogonal basis of the identity representation of the icosahedral capsid shell symmetry group. They are linear combinations of $Y_{l.m}(\theta,\phi)$ with the given *l* which are obtained by the restriction of the O(3) group to the icosahedral group I_h. The number of identity representations n_t is given by the character relation in the form [24]:

$$n_t(l) = 1/|G|\sum_G \xi_l(\hat{g}), \tag{6}$$

where the sum runs over the elements $\hat{g}$ of the I_h symmetry group, $|G| = 120$ is the number of elements in the group, and $\xi_l(\hat{g})$ are the characters of the irreducible representation of O(3) with the fixed l value. Taking into account the fact that all functions with even wave numbers l are invariant with respect to spatial inversion we limit sum (6) to the 60 icosahedron rotations only. After partition of the representation characters into conjugacy classes Eq. (6) takes the following form:

$$n_t(l) = \frac{1}{60}(2l+1+15\xi_l(\pi)+20\xi_l(2\pi/3)+12\xi_l(2\pi/5)+12\xi_l(4\pi/5)), \quad (7)$$

where $\xi_l(\alpha) = \sin((l+1/2)\alpha)/\sin(\alpha/2)$ is the character of the rotation through an angle α matrix.

For an arbitrary surface with the icosahedral shape symmetry I_h displacement field (4) can contain a number of functions $f_l^i(\theta,\varphi)$ with different values of l. However, here we adopt the approach of the Landau theory of phase transitions [25], and assume that the considered shape transformation is driven by a single critical order parameter which spans one irreducible representation. The amplitude of this function with the fixed l gives the main contribution to the capsid free energy variation in the vicinity of the morphological transformation point where the amplitudes of other non-critical components in (4) are negligibly small. Then, the group theory analysis presented above shows that the simplest radial displacement field responsible for the capsid shape symmetry breaking is characterized by the wave number value *l=6*. In Cartesian coordinates the $f_6(x,y,z)$ function has the following simple form:

$$f_6(x,y,z) = (y^2 - z^2\tau^2)(z^2 - x^2\tau^2)(x^2 - y^2\tau^2) - 1/21(\sqrt{5}-2), \quad (8)$$

where $\tau = (\sqrt{5}-1)/2$ is the golden mean, and coordinates <*x, y, z*> of a point on a unit sphere are related in a standard way to θ and φ variables of a spherical coordinate system. Note that two opposite signs of the $f_6(x,y,z)$ function amplitude lead to two different surface shapes with the icosahedral symmetry. The displacement field with the positive amplitude results in a surface with the *icosahedral shape*, while for the opposite sign the surface acquires the *dodecahedral shape* (see Fig. 1). A similar relation was obtained in [20] for tethered spherical networks undergoing buckling transitions. Experimentally, in the case of bacteriophage HK97 considered in our work the capsid shape induced by the displacement field is icosahedral (see Fig. 1,c) [12]. However, there exist a number of viruses which display dodecahedral capsid shape. An example of viruses of this type is given by the pathogenic human Parvovirus B19 (Fig. 1,d) [26]. It is remarkable that the simplest critical function given by Eq. (5) catches this structural difference and describes it in a very simple way.

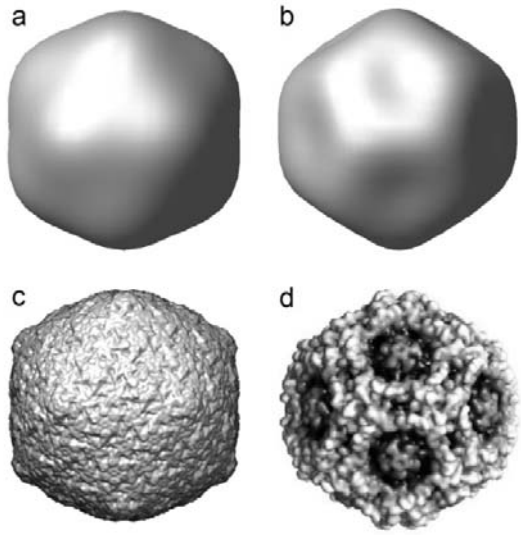

FIG. 1. (a-b): Spherical surface deformation by the radial displacement fields proportional to the icosahedral function $f_6(\theta,\varphi)$. The amplitudes $D_{6,i}$ of the displacement fields in panels (a) and (b) have opposite signs. (c-d): Experimental realization of the capsid shapes induced by displacement fields (a) and (b). Viral capsid of the bacteriophage HK97 [12] with the icosahedral faceted shape (c), and viral capsid of the pathogenic human parvovirus B19 [26] (d) with the dodecahedral faceted shape.

The next step of the symmetry analysis is devoted to shear modes of the spherical membrane. Below we construct explicitly the shear displacement fields with the icosahedral symmetry and show that the simplest of them is responsible for the protein reorganization during the specific intermediate stage of the HK97 maturation, i.e. the EI state formation (see Introduction). This stage results in the symmetrization of the initially skewed hexamers, and is followed by the irreversible cross-linking of capsid proteins [12,27-28].

Displacement fields which correspond to shear modes of the spherical membrane are tangent to the sphere surface and are described by the so-called vector spherical harmonics W_{lm} [29, 22]. These functions have the rotational symmetry similar to that of scalar spherical harmonics Y_{lm} with the same wave number l, but their parity with respect to spatial inversion is opposite to the parity of Y_{lm} functions. Let us present the principle of shear displacement field construction, the selection rules for the shear modes preserving the global icosahedral symmetry of the assembly, and the explicit form of the icosahedral shear displacement field with $l = 6$ responsible on the capsomer deformation.

In order to obtain the icosahedral shear functions we use classical methods similar to those used above for the radial function f_l construction [24]. The form of the shear function is simpler in Cartesian coordinates. The spherical harmonic Y_{ll} with $m=l$ (up to its normalization) reads in Cartesian coordinates as: $Y_{ll}=(x-iy)^l$, where (x,y,z) are the components of a vector. Analogously, the vector harmonic W_{ll} with $m=l$ is a simple function dependent on the components of two different vectors $\mathbf{r}=(x,y,z)$ and $\mathbf{r}'=(x',y',z')$: $W_{ll}=z'(x-iy)^l-z(x'-iy')\,(x-iy)^{l-1}$. Then, all other vector harmonics W_{lm} with m=l-1, l-2,…-l forming the basis of the (2l+1)-dimensional representation with the fixed wave number l are easily obtained by successive

application of the lowering operator [24] $J_- = z(\partial_x + i\partial_y) - (x+iy)\partial_z + z'(\partial_{x'} + i\partial_{y'}) - (x'+iy')\partial_{z'}$ which acts on the **r** and **r'** components.

The rotational symmetry of W_{lm} and Y_{lm} functions being the same, the selections rules for the wave number l value for the radial and the shear icosahedral functions are also the same. Thus, the allowed values of l for the shear functions with the icosahedral symmetry are given by condition (3) obtained previously for the radial fields. The explicit form of the icosahedral shear functions $S_l^i(\mathbf{r},\mathbf{r}')$ with a given fixed l value is readily obtained by the averaging of vector spherical harmonics W_{lm} over the icosahedral symmetry group I:

$$S_l^i = C_l^i \sum_G W_{lm}(\hat{g}(\mathbf{r}), \hat{g}(\mathbf{r}')), \tag{9}$$

where $G=I$ and the coefficients C_l^i can be determined from the normalization and (for $l \geq 30$) from the orthogonality condition for functions (9) with the same l value. Similar to the case of radial icosahedral fields, the icosahedral shear function $S_l(\mathbf{r},\mathbf{r}')$ with the fixed l value obtained by the averaging is unique for $l<30$ and contains no internal fitting parameter. The components of the irreducible shear field **u** with the icosahedral symmetry are then expressed as the derivatives of scalar shear function (9) with respect to the **r**' components:

$$\mathbf{u} = < \partial_{x'} S_l^i, \partial_{y'} S_l^i, \partial_{z'} S_l^i > \tag{10}$$

In the simplest case (i.e. for $l=6$) icosahedral shear field (10) has the following explicit form (up to normalization coefficients):

$$\begin{aligned} u_x &= (-\sqrt{5}\tau x^4 + y^4 + \tau^2 z^4 + 2\sqrt{5}\tau^2 x^2 y^2 - 2\sqrt{5}x^2 z^2 - 2\sqrt{5}\tau y^2 z^2) yz; \\ u_y &= (\tau^2 x^4 - \sqrt{5}\tau y^4 + z^4 - 2\sqrt{5}x^2 y^2 - 2\sqrt{5}\tau x^2 z^2 + 2\sqrt{5}\tau^2 y^2 z^2) xz; \\ u_z &= (x^4 + \tau^2 y^4 - \sqrt{5}\tau z^4 - 2\sqrt{5}\tau x^2 y^2 + 2\sqrt{5}\tau^2 x^2 z^2 - 2\sqrt{5} y^2 z^2) xy. \end{aligned} \tag{11}$$

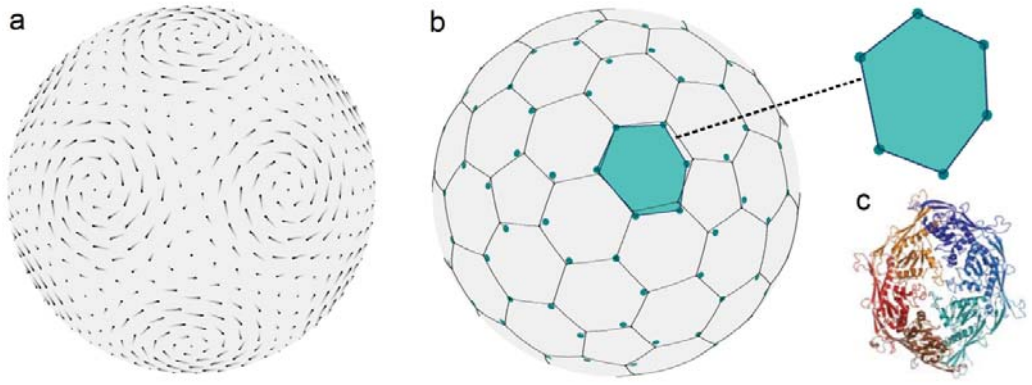

FIG. 2. Simplest irreducible shear field ($l=6$) with the icosahedral symmetry and hexamer deformation in the HK97 procapsid. (a) Shear field on a spherical surface. Vectors of the field are given by segments, segment color intensity gradient indicates vector direction, and segment length is proportional to the field amplitude. For the sake of clarity the amplitude is exaggerated with respect to the sphere size. The field is antisymmetric with respect to spatial inversion. It is invariant with respect to all icosahedron rotations and vanishes at the global icosahedral symmetry axes. With a good accuracy, in the vicinity of the 5-fold axes spherical membrane regions rotate as a whole under the shear field action, amplitude of the field being proportional to the distance from the axis. (b) Global deformation of the sphere tessellation (Caspar-Klug « spherical lattice » triangulation) with T=7 by the icosahedral shear field shown in panel (a).

Structure of the HK97 bacteriophage is commonly interpreted in terms of this tessellation containing 12 pentamers and 60 hexamers. (c) Distorted hexamer shape in the HK97 procapsid (structural data taken from [7]).

Figure 2 shows the relation between icosahedral shear field (11) and the deformation of hexamers observed experimentally at the early stages of the HK97 maturation process. Let us stress that this shear field induces not only hexamer deformations but pentamer rotations also. It is remarkable that the corresponding "twist of pentamers" was observed experimentally [7]. In addition, the angle of the pentamer twist during the HK97 maturation process is approximately equal to the pentagonal tile rotation shown in Fig. 2,b. It is also worth noting that, according to the authors of [7], the sides of pentamers and hexamers in the HK97 capsid are not parallel to each other, making this capsid slightly different from the classical Caspar-Klug structure. Fig. 1,c in [7] shows also that in the HK97 procapsid the side of the deformed hexamer adjacent to the pentamer is not parallel to the corresponding pentamer side. Thus, the difference from the Caspar-Klug structure is inessential; the pentamer twist and symmetrization of the adjacent hexamer are correlated and are described with a good accuracy by the icosahedral shear field given in Figs 2, (a,b). Finally, let us note that the calculated shear field vanishes at the icosahedral 3-fold axes making them local rotation centers. The comparison of the experimental procapsid and capsid structures given in [7] reveals the corresponding "pivots" in the HK97. Due to the global icosahedral symmetry of the shear field all 60 hexamers in the capsid are equivalent. The same concerns the procapsid hexamers. Thus, the local 3-fold axes are shifted only slightly during the morphological transformation.

Resuming this analysis we can say that the capsomers in the HK97 procapsid structure are deformed by the simplest continuous icosahedral shear field. The field is very close to the irreducible (IR number l=6) shear strain mode of the spherical membrane. Though the shear field and radial displacement field (8) have the same wave number l=6 they are linearly decoupled since they have different parity properties with respect to spatial inversion. Therefore, these fields correspond to different independent normal modes of the spherical shell and their overlapping cannot be essential.

To proceed further, let us note that the EI state formation occurs in two steps [12,27-28]. The first of them, the PII <->EI-1 transformation, is reversible [10]. At the irreversible second step cross-linking bonds between the capsid proteins appear. Below, in the frame of the Landau-Ginzburg theory, we construct a simple thermodynamic model of the reversible stage of the maturation process. For the sake of clarity, we consider only the critical degrees of freedom related to the capsid shape variation and described by the radial fields with $l=6$ and $l=0$.

III. FREE ENERGY OF THE PROCAPSID-TO-CAPSID SHAPE TRANSFORMATION

The symmetry and structure analysis performed in the previous Section shows that the main features of the shape variation during the maturation process in the HK97 bacteriophage and in similar viruses are described by the radial displacement fields with the minimal set of spherical harmonics. The critical order parameters span two irreducible representations of the O(3) symmetry group with $l=0$ and $l=6$. The former field is responsible for the isotropic volume changes while the latter one breaks the shape symmetry from the spherical to the icosahedral one. Free energy of the transformation is dependent on the amplitude A_{00} of the fully symmetric function with $l=0$, and 13 amplitudes $A_{6,m}$ of the harmonics with $l=6$.

The Landau free energy dependent on the components of the considered order parameters can describe different low-symmetry states. The number of linearly independent order parameter components in different states is quite different because the linear relations between 13

amplitudes $A_{6,m}$ are strongly dependent on the state symmetry. In the simplest free energy model developed in the present work we are interested not in all transitions into all possible ordered states, but in the spherical-to-icosahedral transition only. To describe this single transformation (and not a system of phase transitions) we apply the well-known method of "effective" order parameter and "effective" free energy widely used in the theory of phase transitions (see e.g. [30,31]). The method reduces the description to linearly independent components of the order parameter. A similar method is applied in [20] to the problem of the spherical tethered network buckling.

In the considered case the symmetry group analysis performed in the previous section shows that in the icosahedral state all 13 amplitudes $A_{6,m}$ are linearly dependent and proportional to a single variable noted below as η. This "effective" order parameter coincides with the amplitude $B_{6,1}$ of the $f_6(\theta,\varphi)$ function in Eq. (4). The "effective" free energy depends only on η and on the variable responsible on the isotropic volume variation. It describes only the transition between the spherical and the icosahedral states. The value of the order parameter η obtained by the free energy minimization defines the degree of the capsid faceting. The sign of η discriminates between the icosahedral and dodecahedral shape of the resulting capsid.

In what follows, instead of the A_{00} amplitude of the fully symmetric harmonic Y_{00} responsible for the isotropic expansion (or compression) we use the capsid's volume variation ΔV as a variable in the free energy expansion. This choice is more suitable for physical interpretation of the results obtained in the frame of the developed approach. It is evident that the amplitude A_{00} and the volume variation ΔV are related linearly. This justifies the change of variable proposed here. Then, the minimal expansion of the free energy density F describing the morphological transformation during the maturation process in the HK97 capsid takes the form:

$$F = A(d)\eta^2 + a_2\eta^3 + a_3\eta^4 - P\Delta V + b\Delta V^2 - |g|\Delta V\eta^2, \qquad (12)$$

The symmetry of the considered problem forbids two terms in free energy density (12). First of all, the term linear in η is absent. This term would make impossible the free energy minimum in the spherical non-faceted state ($\eta=0$). Secondly, free energy density (12) does not contain the bilinear coupling term proportional to the $\eta\Delta V$ product. It is forbidden by the fact that ΔV and η span two different representations of the spherical membrane symmetry group. The phenomenological coefficient $A(d)$ in free energy density (12) is dependent on the capsid shell thickness d, which depends in turn on a number of biochemical parameters. Detailed discussion of the biochemical processes involved in the maturation and corresponding microscopic parameters is out of the scope of the present phenomenological work. Here we focus on the minimal model construction and on the full symmetry analysis of the shape transformation problem. We limit our discussion to the well-established experimental result: a decrease in the capsid shell thickness leads to the faceting transition which is proved to be reversible *in vitro*.

The applicability region of the proposed model for *in vitro* experiments concerns the maturation steps experimentally proved to be reversible, e.g. the Prohead I-to-Expanded Prohead I transition [15] and the Prohead II-to-Expansion Intermediate I transformation [10]. It is evident that genome packaging in *in vivo* experiments is an irreversible process and cannot be described explicitly in the frame of phenomenological theory of phase transitions. However, several physical aspects induced by the genome packaging, e.g. internal capsid pressure variation, can be taken into account phenomenologically.

In the frame of the Landau approach developed in our work the morphological transformation thermodynamics is described by free energy (12). The stability limit for the spherical capsid shape corresponds to the coefficient $A(d)$ vanishing. But the faceting instability transition takes place even earlier, when $A(d)$ is still positive. More detailed analysis shows that

the considered shape transition is discontinuous. The procapsid undergoes the first order faceting transition before the full softening of the normal mode responsible for this shape transition takes place.

The discontinuous character of the faceting transition is directly related to the presence of the cubic term $a_2\eta^3$ in free energy density (12). It is worth noting that any irreducible representation of the O(3) group with *even* value of the wave number l admits an invariant term which is cubic in a function of amplitudes of spherical harmonics. This fact was widely used previously in many different fields of physics. It is the case, for example, of nematic liquid crystal physics [30]. The orientational ordering of rod-like molecules is described by the second-rank symmetric traceless tensor Q_{ij} , and the nematic order parameter spans the irreducible representation of the O(3) group with $l=2$ [30,31]. It is evident that the determinant of the corresponding tensor is the cubic invariant of the irreducible representation. The same principles applied to other values of l show that cubic invariant exists for all even wave numbers. Direct calculation of the cubic invariant for the irreducible representation with $l=6$ can be performed explicitly using properties of Clebsch-Gordan coefficients [24,32]. Because of its cumbersome form, we omit it in the present work. Note, that the cubic term in the free energy is not only responsible for the discontinuous character of the transition, but also plays the crucial role in the choice between the icosahedral and the dodecahedral shapes of the resulting capsid shell.

Other terms of free energy density (12) have a rather straightforward form and physical meaning. Because of the identical symmetry of the mode responsible for the isotropic volume change the free energy contains the term which is linear in ΔV and the coupling term which is quadratic in the symmetry-breaking order parameter η and linear in ΔV. The term quadratic in ΔV with the positive coefficient $b>0$ ensures the global stability of the isotropic expansion (or compression) mode. The fourth-degree term in powers of the order parameter η with the positive coefficient $a_3>0$ ensures the existence of a global minimum in the considered system. The coefficient P in free energy density (12) expresses the pressure difference between the inner and the outer regions of the capsid shell. In a more complex model it is possible to take into account higher non-linearity of the free energy in a function of the isotropic expansion (or compression) mode represented here by the variable ΔV. Nonlinear in ΔV terms would favor intermediate states between the spherical procapsid and the icosahedral capsid. But in the minimal model of the shape transformation these terms lead to unjustified mathematical complications.

The minimization of the free energy functional with the density given by (12) leads to three possible solutions with different symmetries: i) $\eta=0$; ii) $\eta<0$; and iii) $\eta>0$, volume change ΔV being nonzero for all three states. Solutions ii) and iii) with opposite signs of the order parameter correspond to the shell with the icosahedral and the dodecahedral shape, respectively. They are usually called anti-isostructural states in the theory of phase transitions in condensed matter [30]. The free energy density being non-linear in η and quadratic in ΔV, it is more convenient to minimize it first with respect to ΔV, and then substitute the solution in (12). Simplified in this way, free energy (10) depends only on the symmetry breaking order parameter η and its minimization yields the values of η in both the icosahedral and the dodecahedral states of the shell:

$$F(\eta) = (A(d) - |g|P/(2b))\eta^2 + a_2\eta^3 + (a_3 - g^2/(4b))\eta^4 - P^2/(4b), \qquad (13)$$

In free energy density (13) the pressure increase induced by the genome packaging into the capsid shell contributes to the variation of the phenomenological coefficient multiplying the term quadratic in order parameter η. Negative sign of the term with $|g|$ corresponds to the fact that the packaging-induced growth of internal pressure leads to the capsid volume increase and favors the shape transformation. Shell faceting could be then favored not only by the experimentally observed capsid shell thinning, but by an eventual internal pressure increase also. Let us stress that besides the capsid shell thinning, the factors which influence shell faceting are still not

elucidated experimentally. In addition to the increase of the internal pressure these could be other physical mechanisms, e.g. surface interaction between the inserted genome and the capsid proteins leading to the conformational changes in coat proteins. In the present model the degree of shell faceting is determined by the equilibrium value of the order parameter η. Thus, the model predicts that the degree of shell faceting grows with the shell wall decrease and the internal pressure increase according to the law:

$$\eta = \frac{-6a_2 - \sqrt{9a_2^2 - 16(\mathrm{A(d)} - |\,\mathrm{g}\,|\,\mathrm{P}/(2\mathrm{b}))(a_3 - g^2/(4b))}}{8(a_3 - g^2/(4b))}.$$

The phase diagram of the model is presented in Fig. 3. Free energy (13) graphs for several typical points in the phase diagram are given in inserts a), b) and c) in Fig. 3. The points are taken in the corresponding regions in the phase diagram. The phase diagram shows that the in-out pressure difference variation and the *A(d)* coefficient variation, induced by the shell thinning and by the pH level decrease, contribute to the same part of the free energy.

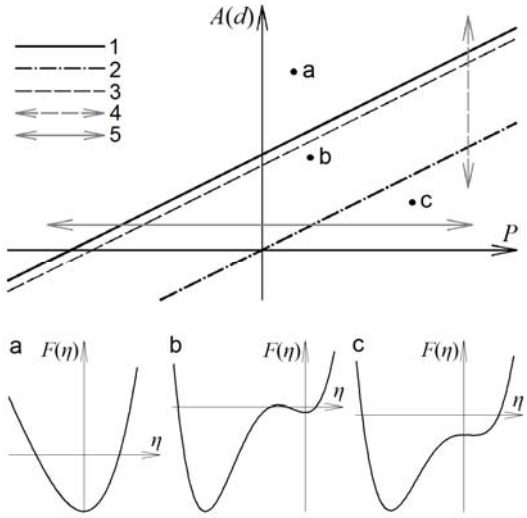

FIG. 3. Phase diagram of the free energy functional with density (12). Full line 1 and dash-dotted line 2 divide the phase diagram in qualitatively different regions: the region of stability of the minimum with the spherical symmetry, the region of stability of the minimum with the icosahedral symmetry, and the region where two minima with different symmetries coexist. The minimum with η=0 (spherical shape state without faceting) exists only in the region above line 2. The state with the icosahedral shape (η<0) appears below line 1. At dashed line 3 free energies of the spherical and the icosahedral faceted states are equalized. Below line 2 the minimum which corresponds to the spherical state disappears. It is replaced by the weak metastable minimum with η<0. Inserts a), b) and c) show free energy density (13) as a function of the order parameter η in several typical points. Corresponding points are given by the same letters in the phase diagram. Two qualitatively different thermodynamic paths of the morphological transformation are shown by arrowed lines. Line 4 (downward) corresponds to the shell thinning induced by the pH level decrease. Line 5 (from left to right) illustrates the result of the pressure difference increase. During the *in vivo* genome packaging into the capsid the thermodynamic path of the system passes between lines 4 and 5 and corresponds to the simultaneous capsid shell thinning and internal capsid pressure increase.

The phase diagram in Fig. 3 was calculated for the case a_2>0. For negative values of this coefficient, each graph of free energy density (13) in inserts a), b) and c) is reflected with respect to the *F* axis. With this change of the sign the ordered state with the icosahedral symmetry

changes its shape from the icosahedral to the dodecahedral one. Corresponding lines in the phase diagram separate in this case the regions of stability of the spherical and the dodecahedral shell shapes. Dashed line 3 indicates in this case the first-order transition between the spherical and the dodecahedral states.

The minimal model of the shape transition developed here allows us to calculate analytically the equation of line 3 where the free energies of the spherical and the icosahedral (or dodecahedral) states become equal:

$$A(d) = \frac{1}{2}\frac{4Pa_3bg - Pg^3 + 2a_2^2b^2}{(4a_3b - g^2)b}$$

Another important quantitative characteristic which is also obtained analytically in the frame of the minimal model is the value of the volume jump at the discontinuous transition from the spherical to the faceted state:

$$\Delta V = \frac{1}{8}\frac{g(3ba_2 + \sqrt{9a_2^2b^2 - 32a_3b^2A(d) + 16a_3bgP + 8g^2bA(d) - 4Pg^3})}{(4a_3b - g^2)^2b}$$

IV. DISCUSSION AND CONCLUSION

We have analyzed three collective displacement modes responsible for the morphological changes taking place during the maturation process in capsids of the HK97 bacteriophage and similar viruses. In the continuous approximation all three modes correspond with a good accuracy to the simplest irreducible deformation fields of a spherical shell. We have shown that the continuous approximation describes not only the capsid faceting and volume variation, but also the capsid hexamer symmetrization and pentamer rotations [7,33]. In *in vitro* experiments the shape transition is followed by the irreversible cross-linking of the capsid proteins [12, 27-28]. The reversible shape transformation, at the preceding stage of the maturation process, results in a capsid faceting and expansion. We construct a thermodynamic Landau-Ginzburg model of the corresponding shape transition. The model establishes the relation between the faceting transition and two external thermodynamic parameters of the system. First of them is the capsid shell thinning induced by the pH level decrease, observed in *in vitro* experiments. The second one is connected to the pressure difference increase between the inner and outer regions of the shell. During the i*n vivo* virus maturation process, a progressive genome packaging into the capsid shell with the help of motor proteins leads to the pressure difference increase. Here we show that the *in vivo* shell faceting could be favored not only by the experimentally observed capsid shell thinning but by the internal pressure increase also.

In our work we developed for the capsid maturation transition the idea [16] of critical mode selection. Both our theory and the approach proposed in [16] are based on the Landau's ideas about critical degrees of freedom playing a key role during structural phase transitions. Let us stress that, in contrast to [16] we use a continuous model of the capsid and perform a detailed symmetry analysis of the structural data obtained in [7], which were published after the publication of [16]. As a consequence, we distinguish the critical modes partially different from those proposed in [16]. In our opinion, these modes are more suitable to account for the experimentally observed variation of the HK97 capsid structure during its maturation process.

The capsid shape transformation mechanism proposed in our work is consistent with classical works [34,35] on the capsid shell faceting based mainly on the continuum elasticity theory. These works have used the analogy between the faceting phenomenon and the longitudinal instability of disclinations in two-dimensional crystals. They have shown that in the locally hexagonal protein packing, proposed as a model for viral capsid organization by Caspar and Klug [5], disclination instabilities in the vicinity of five-fold axes lead to the capsid faceting for viruses of sufficiently big size. The model proposed in [34] was based on the non-linear

physics of thin elastic shells. It analyzed the shell buckling instability and elucidated the dependence of the viral capsid faceting on the value of a dimensionless Föppl–von Kármán (FvK) number γ. The FvK number is the combination $\gamma=YR^2/\kappa$, where Y is the two-dimensional Young modulus of the shell, κ is its bending rigidity, and R is the mean radius of the capsid shell [34]. High bending rigidity favors smooth, practically spherical shell shape while low bending rigidity leads to the faceted shape. In the model developed in our work the capsid shell thinning is shown to be one of the two important external thermodynamic parameters of the shape transformation. It is evident that the shell thinning results in the decrease of its bending rigidity κ. The decrease in κ leads to the shell faceting in good agreement with the predictions of [34]. To complete the approach [34,35] we took into account the experimentally observed increase in the capsid average radius and the shell volume during the HK97 maturation process [27].

The capsid faceting phenomenon was also a subject of numerical modeling based on the simplified interaction potentials of capsomers taken as interacting particles. Recent work [19] considered both spherical and faceted states in the frame of the simplest inter-capsomer Lennard-Jones pair potential for several viruses satisfying Capsar and Klug selection rules. The pair potential put in the basis of this work conserves the average distance between the capsomers, and, consequently, makes the surface areas of the spherical and the faceted capsids approximately equal. This condition makes, in turn, the radius of a sphere circumscribed around the faceted capsid greater than the radius of the spherical one while the volume of the faceted capsid decreases. Though mathematically such a model is self-consistent, its geometric properties differ greatly from the experimentally observed increase in both the average capsid radius and the capsid volume during the maturation process in the HK97 and similar viruses.

In recent work [18] the classical approach developed in [34,35] was submitted to a certain criticism. The continuous elastic model developed in [18] proposed to relate the faceting transition not to the FvK number but to the hexamer shape variation. However, the X-ray crystallography and the high-resolution cryoEM data reveal one more intermediate state of the HK97 maturation process which is characterized by the spherical capsid shape and the regular symmetric hexamer shape simultaneously [11]. Thus, we consider that the hexamer shape variation is not directly related to the capsid shell faceting. By contrast, further development of the shape transition theory in spherical shells with the fixed highly symmetric positions of disclinations [20] seems to us very interesting and promising. We expect that in the near future it will be possible to construct a micromechanical model of such a shell which admits the simplest shear mode (Fig. 2,a) as a critical order parameter for the shell "torsion" preserving its icosahedral symmetry.

We also expect that the progress in the cryoEM technique will soon result in new high-resolution data on the intermediate states of the HK97 morphological transformation. These additional data would constitute the basis for the further development of the minimal model proposed in the present work. The simplest extension would be the model which takes into account in (12) the terms of higher order in ΔV. It is easy to see that by adding the fourth–order terms in ΔV in (12) one obtains additional states which differ by the shell volume values. They might correspond to several spherical shells with different volumes observed in *in vitro* experiments [3,7,36].

In conclusion, let us note that the minimal thermodynamic model with a clear physical meaning of the free energy parameters proposed in the present work describes the viral capsid shape transformation during the maturation process in the HK97 bacteriophage and in similar viruses. The underlying physical processes are driven by the order parameters spanning irreducible representations of the O(3) symmetry group, which characterizes the procapsid macroscopic spherical shape. The considered morphological transformation during the maturation process is understood as a phase transition leading to the isotropic shell expansion and the symmetry-breaking faceting. The first fully symmetric order parameter is related to the

shell volume change ΔV. The second 13-dimensional order parameter responsible for the procapsid shape symmetry breaking describes explicitly the icosahedral faceting of the viral shell. It spans the even irreducible representation of the O(3) group with $l=6$ and represents the linear combination of the spherical harmonics with $l=6$ invariant with respect to the icosahedral symmetry group I_h. In the state with the icosahedral symmetry all 13 components of this order parameter depend on only one amplitude. In the minimal model of the transformation this fact is described by the effective one-dimensional order parameter η. The model is then reduced to the coupling between the fully-symmetric order parameter responsible for the capsid volume change and the one-dimensional order parameter responsible for the shell faceting. It admits third-order term in η in the free energy, thus making the morphological transformation discontinuous. The sign of the third-order term discriminates between the icosahedral and the dodecahedral shapes of the faceted capsid. The calculated phase diagram shows two qualitatively different paths of the transformation in a function of the main external thermodynamic parameters of the *in vitro* and *in vivo* experiments and the possibility of simultaneous variation of these parameters. The ensemble of the results obtained describes the experimentally observed physical phenomena which accompany the maturation process in the HK97 bacteriophage and similar viruses.

APPENDIX: DISPLACEMENT FIELDS WITH THE ICOSAHEDRAL SYMMETRY ON A SPHERICAL SURFACE

The analysis performed in terms of the invariant theory makes it possible to construct an arbitrary function with the icosahedral symmetry. It provides a justification for selection rules (3) which determine the possible wave numbers l associated with the order parameter of the faceting transition. This order parameter is responsible for the procapsid shape symmetry breaking from O(3) to I_h.

We start with the properties of an arbitrary scalar function defined on a spherical surface (e.g. a function of radial displacements of the capsid shell material points) and invariant with respect to the symmetry group I_h, which contains all symmetry operations of an icosahedron. Let us fix the point group orientation with respect to the coordinate frame and choose Cartesian axes $\boldsymbol{x}$, $\boldsymbol{y}$ and $\boldsymbol{z}$ along the two-fold symmetry axes of the icosahedron. This choice allows us to express the invariants of the full icosahedral group in a simple way. Another property of the group helps us to construct the so-called integrity basis constituted by the generators of the ring of invariant polynomials. Any function with the icosahedral symmetry can then be expanded in series of the finite number of invariant polynomials constituting the integrity basis. The point group I_h belongs to the class of simple mathematical objects called groups generated by reflections. For the groups of this type the number of invariants in the integrity basis is equal to the dimension of its vector representation (i.e. to the dimension of the space in the considered case) and the product of degrees of basis invariants is equal to the number of the group elements $|G|$. Consequently, the integrity basis of the I_h group contains only three following invariant polynomials with the degrees 2, 6 and 10, respectively:

$$J_0 = x^2 + y^2 + z^2, J_1 = \prod_{i=1}^{6} \mathbf{q}_i \mathbf{r}, J_2 = \prod_{i=1}^{10} \mathbf{p}_i \mathbf{r} \ , \qquad (11)$$

here $\mathbf{r} =< x, y, z >$; vectors $\mathbf{q}_i$ and $\mathbf{p}_i$ are parallel to the 5-fold and 3-fold icosahedral axes, respectively. From the geometric point of view each term in the products in the expressions for the invariant polynomials J_1 and J_2 is equivalent to the equation of a plane perpendicular to the 5-fold and 3-fold axes.

According to the well-known presentation of spherical harmonics as homogeneous polynomial functions, any icosahedral function f_l (given by Eq. (5)) with the fixed wave number

l can be expressed as a homogeneous polynomial in $\mathbf{r} =< x, y, z >$ of the degree l. Taking unit radius-vector length we express **r** in spherical coordinates as:

$$x = \sin\theta\cos\varphi\,,\ y = \sin\theta\sin\varphi\,,\ z = \cos\theta\,.$$

On the unit sphere the invariant J_0 acquires constant value J_0=1. Then, any function on a spherical surface invariant with respect to the icosahedral symmetry group I_h can be presented in the form:

$$f_l(\theta,\phi) = A_0 + A_1 J_1 + A_2 J_2 + A_3 J_1^2 + A_4 J_1 J_2 + A_5 J_1^3 + A_6 J_2^2 \ldots \quad (12)$$

The degree l of the f_l function (as a function of the radius-vector components) is equal to the degree of the last terms in expansion (12). The number of terms of the degree l in (12) is the number of possible integer linear combinations of numbers 6 and 10 equal to l. Consequently, for any homogeneous function of the degree l invariant with respect to the I_h group, the number l satisfies to the condition l=6i+10j, where i and j are non-negative integers.

Due to the function irreducibility, the coefficients A_i multiplying the terms with the degrees smaller than l in (12) are univocally defined by the orthogonality of function (12) to the basic functions of other irreducible representations with the wave numbers $l'<l$. The following orthogonality relations hold for a given irreducible function F:

$$\iint F(\theta,\phi) Y_{l'm} \sin\theta d\phi d\theta = 0, \text{for all } l' < l \quad (13)$$

In practice, the number of equations in system (13) is much higher than the number of unknown coefficients in function (12). However, the additional equations are either linearly equivalent or become identities.

Author contribution statement and Acknowledgments

V.L. proposed to develop the Landau-Ginzburg theory for the study of maturation process in viral capsids. S.R. proposed the explicit method for the icosahedral shear deformation field construction. O.K. interpreted the hexamer deformation and pentamer twist in the HK97 capsids as a simplest icosahedral shear field. Authors contributed equally to all other results presented in the paper.

S.R. and O.K. acknowledge financial support of Russian Science Foundation (grant number 15-12-10004). V.L. acknowledges financial support by the Laboratory of Excellence NUMEV (France), partial support by National Science Foundation Grant No. PHYS-1066293 and the hospitality of the Aspen Center for Physics.

References

[1] S. J. Flint, L. W. Enquist, V. R. Racaniello, and A. M. Skalka, *Principles of Virology: Molecular Biology, Pathogenesis, and Control* (ASM, Washington, 2000); J.B. Bancroft, *Advances of Virus Research* (Academic, New York, 1970), Vol. 16, p. 99.

[2] J. King and W. Chiu, in *Structural Biology of Acknowledgments Viruses*, edited by W. Chiu, R.M. Burnett, and R. Garcea (Oxford University Press, New York, 1997), p. 288.

[3] J.F. Conway, W.R. Wikoff, N. Cheng, R.L. Duda, R.W. Hendrix, J.E. Johnson, and A.C. Steven, Science **292**, 744 (2001).

[4] L. Li, S. Lok, I. Yu, Y. Zhang, R.J. Kuhn, J. Chen, and M.G. Rossmann, Science **319**, 1830 (2008); I. Yu, W. Zhang, H.A. Holdaway, L. Li, V.A. Kostyuchenko, P.R. Chipman, R.J. Kuhn, M.G. Rossmann, and J. Chen, Science **319**, 1834 (2008).

[5] D.L.D. Caspar and A. Klug, Cold Spring Harbor Symp. Quant. Biol. **27**, 1 (1962).

[6] R.L. Duda, J. Hempel, H. Michel, J. Shabanowitz, D. Hunt, and R.W. Hendrix, J. Mol. Biol. **247**, 618 (1995); W.R. Wikoff, L. Liljas, R.L. Duda, H. Tsuruta, R.W. Hendrix, and J.E. Johnson, Science **289**, 2129 (2000).

[7] I. Gertsman, L. Gan, M. Guttman, K. Lee, J.A. Speir, R.L. Duda, R.W. Hendrix, E.A. Komives, and J. E. Johnson, Nature **458**, 646 (2009).

[8] J.E. Johnson, Curr. Opin. Struct. Biol. **20**, 210 (2010); C.M. Teschke, and K.N. Parent, Virology **401**, 119 (2010).

[9] C. Helgstrand, W.R. Wikoff, R.L. Duda, R.W. Hendrix, J.E. Johnson, and L. Liljas, J. Mol. Biol. **334**, 885 (2003).

[10] R. Lata, J.F. Conway, N. Cheng, R.L. Duda, R.W. Hendrix, W.R. Wikoff, J.E. Johnson, H. Tsuruta, and A.C. Steven, Cell **100**, 253 (2000).

[11] W.R. Wikoff, J.F. Conway, J. Tang, K.K. Lee, L. Gan, N. Cheng, R.L. Duda, R.W. Hendrix, A.C. Steven, and J.E. Johnson, J. Struct. Biol. **153**, 300 (2006).

[12] G. Cardone, R.L. Duda, N. Cheng, L. You, J.F. Conway, R.W. Hendrix, and A.C. Steven, MBio. **5**, e02067 (2014).

[13] L. Gan,J. A. Speir, J. F. Conway, G. Lander, N. Cheng, B. A. Firek, R. W. Hendrix, R. L. Duda, L. Liljas, and J. E. Johnson, Structure 14, 1655 (2006).

[14] P.D. Ross, N. Cheng, J.F. Conway, B.A. Firek, R.W. Hendrix, R.L. Duda, and A.C. Steven, EMBO J. 24, 1352 (2005).

[15] P.D. Ross, J.F. Conway, N. Cheng, L. Dierkes, B.A. Firek, R.W. Hendrix, R.L. Duda, and A.C. Steven, J. Mol. Biol. 364, 512 (2006).

[16] F. Tama and C. L. Brooks III, J. Mol. Biol. **345**, 299 (2005).

[17] T. Guérin and R. Bruinsma, Phys. Rev. E **76**, 061911 (2007).

[18] A. Aggarwal, J. Rudnick, R.F. Bruinsma, and W.S. Klug, Phys. Rev. Lett. **109**, 148102 (2012).

[19] M. Aznar, A. Luque, and D. Reguera, Phys. Biol. **9**, 036003 (2012).

[20] E. H. Yong, D.R. Nelson, and L. Mahadevan, Phys. Rev. Lett. **111**, 177801 (2013).

[21] V. L. Lorman and S. B. Rochal, Phys. Rev. Lett. 98, 185502 (2007); V. L. Lorman and S. B. Rochal, Phys. Rev. B 77, 224109 (2008).

[22] S.B. Rochal, V.L. Lorman, and G. Mennessier, Phys. Rev. E **71**, 021905 (2005).

[23] J.L. Birman, *Theory of Crystal Space Groups and Lattice Dynamics: Infra-Red and Raman Optical Processes of Insulating Crystals* (Springer-Verlag, Heidelberg, 1974)

[24] J. P. Elliot and P. G. Dawber, *Symmetry in Physics* (Macmillan, London, 1979).

[25] L.D. Landau and E.M. Lifshitz, *Statistical Physics*, 3rd ed. (Pergamon Press, Oxford, 1980).

[26] B.L. Gurda et al., J. Virol. **84**, 5880 (2010).

[27] D. Veesler, J. Quispe, N. Grigorieff, C. S. Potter, B. Carragher, and J. E. Johnson, Structure **20**, 1384 (2012).

[28] D. Veesler, R. Khayat, S. Krishnamurthy, J. Snijder, R. K. Huang, A. J.R. Heck, G. S. Anand, and J. E. Johnson, Structure **22**, 230 (2014).

[29] E. L. Hill, Am. J. Phys. **22**, 211 (1954).

[30] Yu. M. Gufan, *Structural Phase Transitions* (Nauka, Moscow, 1982); J. C. Tolédano and P. Tolédano, *The Landau Theory of Phase Transitions* (World Scientific, Singapore, 1987).

[31] P.G. de Gennes and J. Prost, *The physics of Liquid Crystals* (Clarendon, Oxford, 1993); M. Kleman and O.D. Lavrentovich, *Soft Matter Physics. An Introduction* (Springer, Berlin, 2003).

[32] C. Zemach, *Mathematics of Fluid Mechanics*, in *Handbook of Fluid Mechanics*, Ed. by R.W. Johnson (CRC Press, New York, 1998).

[33] A. C. Steven, J. B. Heymann, N. Cheng, B. L. Trus, and J. F. Conway, Curr. Opin. Struct. Biol.**15,**:227 (2005).

[34] J. Lidmar, L. Mirny, and D. R. Nelson, Phys. Rev. E **68**, 051910 (2003).

[35] M. Widom, J. Lidmar, and D. R. Nelson, Phys. Rev. E **76**, 031911 (2007).

[36] K. K. Lee, L. Gan, H. Tsuruta, C. Moyer, J. F. Conway, R. L. Duda, R. W. Hendrix, A. C. Steven, and J. E. Johnson, Structure **16**, 1491 (2008).